Porosity Effects on Catalytic Char Oxidation

Part II: Experimental Results

Oxidation rates of Na_2CO_3- and K_2CO_3-impregnated char samples were measured in an isothermal kinetic control regime. The results were analyzed by a previously developed model to extract the intrinsic catalytic reactivities, freed from superimposed noncatalytic and structural effects. Although the overall catalyzed rates are only several times greater than their uncatalyzed counterparts, the intrinsic catalytic rates were found to be four orders of magnitude greater. The results further indicate that the function of the catalyst is to increase the number of active sites without affecting the activation energy. The overall reaction kinetics are demonstrated to contain the combined contributions of both catalytic and noncatalytic reactions, and in this context the effects of multiple catalysts as well as of the pore structure development during reaction can be understood and interpreted.

J. L. SU and D. D. PERLMUTTER

Department of Chemical Engineering
University of Pennsylvania
Philadelphia, PA 19104

SCOPE

Six char samples impregnated by solutions with different concentrations of Na_2CO_3 and K_2CO_3 were reacted with oxygen in the kinetic control regime, and the reaction rates obtained were analyzed by a previously developed model. The superimposed internal noncatalytic and external catalytic contributions to the overall rate were determined individually, and the intrinsic catalytic activities analyzed to extract the kinetic parameters: reaction order, activation energy, and prexponential factors. The effects of multiple catalysts were examined, as were also the pore structures developed during the catalytic reactions.

CONCLUSIONS AND SIGNIFICANCE

Using a previously derived model, systematic analyses of a series of results obtained at different reaction temperatures with different amounts of catalyst uptake lead to the following observations: (1) the overall catalytic rates are the combined contributions of catalytic and noncatalytic parts, (ii) the intrinsic catalytic activities are bound four orders of magnitude greater than the noncatalytic, (iii) the increases of preexponential factors can be correlated linearly with the surface concentrations of catalyst, and (iv) the activation energies are the same for both catalytic and noncatalytic gasification. It may be concluded that the function of the catalyst on the char is to increase the number of sites on which reaction takes place.

The structural changes in chars that take place during catalytic oxidation show that after partial conversion pore structures were less developed for those samples with greater catalyst uptake, indicating that the predominant reaction takes place on particle exteriors where catalyst was deposited. This finding is consistent with the catalyst deposition model used here. The effects of multiple catalysts on the reaction rates also agree with the predictions of the model on the basis that only those portions of the overall reaction rates contributed by catalytic reaction are additive.

INTRODUCTION

Prior work (Su and Perlmutter, 1985) presented evidence that chars impregnated with inorganic catalysts from solution had catalysts deposited only on char particle exteriors without significant effects on the particle internal pore structure. A model was formulated to describe the reaction kinetic of chars catalyzed in this manner, in which the overall reaction kinetics are the combined

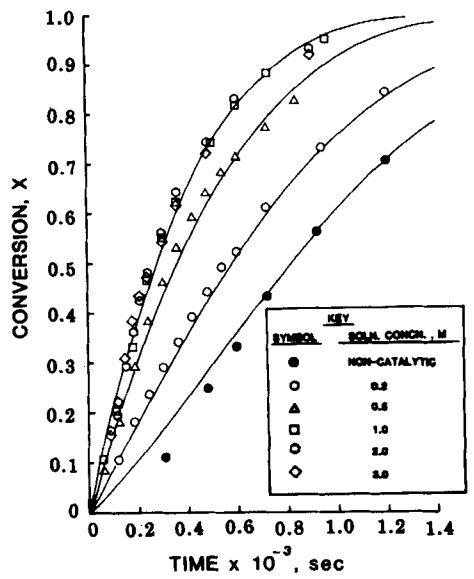

Figure 1. Conversion-time behavior at 400°C for sample *B* impregnated by Na_2CO_3 solution of different concentrations; curves are fitted by the model.

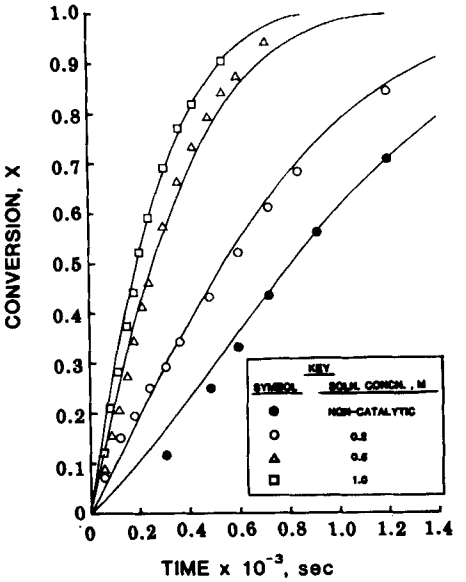

Figure 2. Conversion-time behavior at 400°C for sample *B* impregnated by K_2CO solution of different concentrations; curves are fitted by the model.

contributions of both catalytic and noncatalytic reactions. The model makes it possible to separate these contributions in order to obtain and interpret the intrinsic catalytic reactivities, making use of the conversion and rate relationships:

$$X = 1 - \exp\left[-\tau\left(1 + \frac{\psi\tau}{4}\right)\right]\left[1 - \frac{\alpha\tau}{\sigma}\right]^3 \quad (1)$$

and

$$\frac{dX}{d\tau}\left[3\frac{\alpha}{\sigma} + \left(1 + \frac{\psi}{2}\tau\right)\left(1 - \frac{\alpha}{\sigma}\tau\right)\right] \times \left(1 - \frac{\alpha}{\sigma}\tau\right)^2 \exp[-\tau(1 + \psi\tau/4)] \quad (2)$$

where

$$\psi = \frac{4\pi L_o}{(1 - \epsilon_o){S_o}^2} \quad (3)$$

and

$$\sigma = \frac{R_o S_o}{(1 - \epsilon_o)} \quad (4)$$

This paper reports results of experiments conducted on catalyzed char-air reactions with the object of testing the applicability of the previously developed model. The superimposed internal and external contributions to the overall rate are determined individually, and the intrinsic catalytic activities are analyzed to extract kinetic parameters such as reaction order and activation energy. The effects of multiple catalysts are considered, as well as the pore structure developed during the catalytic reactions.

EXPERIMENTAL

Techniques were described in an earlier report (Su and Perlmutter, 1985) for char sample preparation and catalyst impregnation, as well as for measurement of catalyst uptake and pore structure. Results were also presented giving numerical details on a series of prepared samples. In the work to be reported here the reactivities of these same impregnated samples were measured with a Dupont model 91 thermogravimetric analyzer (TGA). The reaction chamber containing the char sample was purged with nitrogen for 30 minutes and the temperature was then rapidly raised to the desired level for reaction. There was no detectable weight loss in the nitrogen atmosphere for at least one hour, and the duration of this prereaction period did not affect the subsequent rate of the char-air reaction. The reaction was initiated by introducing high purity, dried air at a controlled flow of 100 mL/min. The air temperature, the sample weight, and the time derivative of weight loss were monitored and recorded. As needed the air was diluted with nitrogen to obtain the desired oxygen partial pressure.

Since the reaction is highly exothermic, extreme care had to be taken to minimize the effect of heat and mass transfer in the particle bed. To this end a minimum amount of sample (about 5 mg) was spread uniformly on the sample pan to form a monolayer bed of 250 micron-diameter particles. Under such conditions, it was shown by Su (1983) that the maximum temperature difference between the particle surface and the surrounding gas flow did not exceed 5 K, except for one sample (sample *B* impregnated by 1.0 M K_2CO_3 solution) for which the temperature rise was estimated to be 6.3 K. To prepare partially reacted samples for structural analysis, the reaction was terminated at the desired conversion levels by purging nitrogen through the reaction chamber. TGA results showed that weight loss can be stopped within one minute. The samples were removed from the furnace and cooled under a nitrogen atmosphere.

RESULTS AND DISCUSSION

Reaction Rates

Reaction rates were measured at several reaction temperatures, selected to insure that the interior noncatalytic reactions were in the chemical kinetic control regime. The temperature ranges appropriate for this purpose were chosen by examining data on noncatalytic reaction previously reported (Su and Perlmutter, 1984). Since the catalysts deposited on the particle exterior, there was also no intraparticle diffusion resistance for the catalytic reactions.

Typical results for catalytic char-air reactions are shown in Figures 1 and 2 in terms of conversion-time behavior at 673 K. The corresponding rate-conversion data are shown in Figures 3 and 4. These results were all obtained for the same char sample, but differ according to the catalyst and the concentration of the impregnating solution. As expected from the prior study cited above, the enhanced rates appeared at an early stage of reaction and decreased

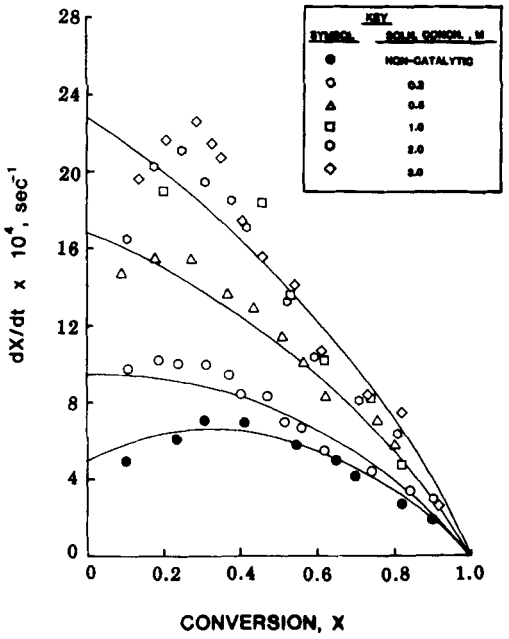

Figure 3. Char-air reaction rates at 400°C for sample *B* impregnated by Na_2CO_3 solution of different concentrations; curves are fitted by the model.

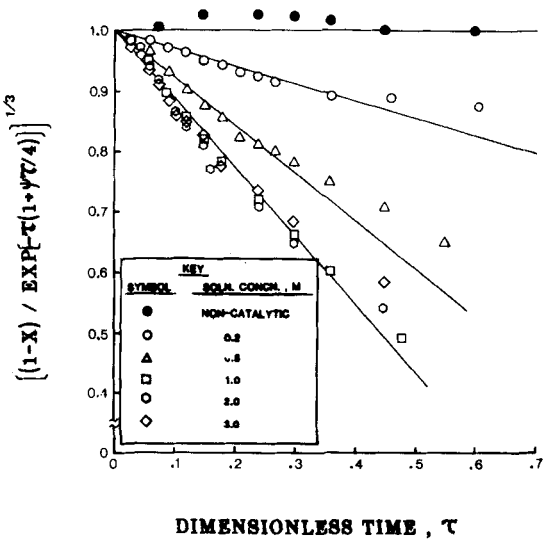

Figure 5. Replotted conversion-time data for char-air reactions of Na_2CO_3-impregnated sample *B* at 400°C.

at higher conversions to those found for noncatalytic reactions. For the same concentration of treating solution, K_2CO_3 showed a slightly greater catalytic effect than Na_2CO_3. Increasing Na_2CO_3 solution concentration from 0.2 M to 1.0 M caused significant rate increases. Higher concentrations of 2.0 M or 3.0 M do not however, further increase the reaction rate. This behavior agrees with the results of the atomic absorption analyses presented by Su and Perlmutter (1985) which show no further catalyst uptake for concentrations higher than 1.0 M.

Following the expectation of Eq. 1, the kinetic data presented above are examined in Figures 5 and 6 on coordinates that produce linear variation. The noncatalytic rate constants k_s required in computing τ were available from the prior study of Su and Perlmutter (1984), and the values of ψ were taken from the direct pore structure measurements in the same source. The straight lines shown in the figures correlate the experimental data up to at least 70% conversion with correlation coefficients >0.98, indicating that α remained essentially constant over this wide range of conversions. In some cases the slope leveled off slightly at higher conversions, suggesting a deactivation of catalyst that is probably due to the loss of contacts between the catalyst and the char surface.

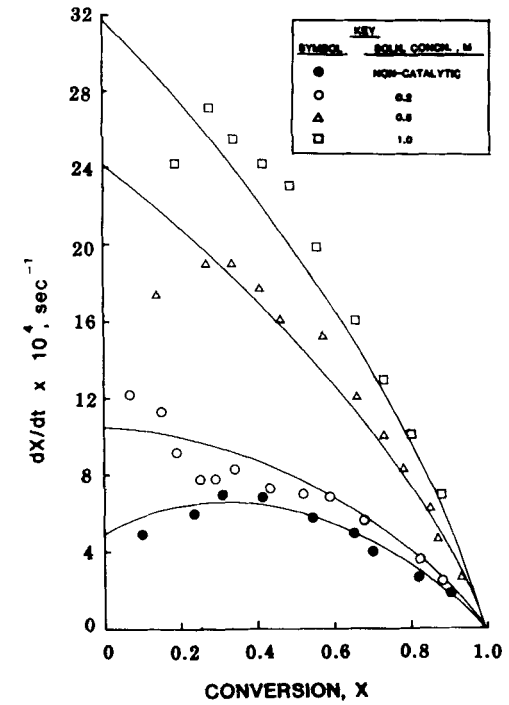

Figure 4. Char-air reaction rates at 400°C for sample *B* impregnated by K_2CO_3 solution of different concentrations; curves are fitted by the model.

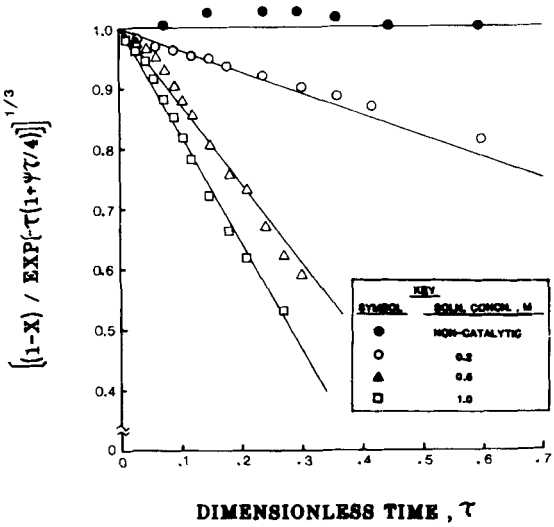

Figure 6. Replotted conversion-time data for char-air reactions of K_2CO_3-impregnated sample *B* at 400°C.

Table 1. Intrinsic Catalytic Rates for Catalytic Char-Air Reactions

Sample	Catalyst	Impregnating Concentration (Molarity)	Intrinsic Catalytic Rates $\times 10^4$, $\frac{g \text{ of } C}{m^2 \cdot s}$ Reaction Temperature, °C 380	400	430	455	480	500
A	Na_2CO_3	1.0	—	—	3.3	7.8	12.8	14.6
A	K_2CO_3	1.0	—	—	21.2	25.9	54.7	63.6
B	Na_2CO_3	0.2	7.5	14.3	22.7	—	—	—
B	Na_2CO_3	0.5	25.6	58.4	103.6	—	—	—
B	Na_2CO_3	1.0	40.0	83.6	136.3	—	—	—
B	Na_2CO_3	2.0	40.0	83.6	136.3	—	—	—
B	Na_2CO_3	3.0	40.0	83.6	136.3	—	—	—
B	K_2CO_3	0.2	20.4	26.6	58.2	—	—	—
B	K_2CO_3	0.5	53.2	94.6	159.0	—	—	—
B	K_2CO_3	1.0	83.2	131.2	245.6	—	—	—
C	Na_2CO_3	0.2	—	13.7	39.1	81.1	—	—
C	Na_2CO_3	0.5	—	18.8	45.9	124.0	—	—
C	Na_2CO_3	1.0	—	32.2	91.8	178.0	—	—
D	Na_2CO_3	0.2	—	9.0	23.6	47.9	—	—
D	Na_2CO_3	0.5	—	17.2	42.5	73.2	—	—
D	Na_2CO_3	1.0	—	23.6	65.1	92.4	—	—
E	Na_2CO_3	1.0	39.0	74.9	119.2	—	—	—
F	Na_2CO_3	1.0	30.8	46.6	88.5	—	—	—

Equation 1 predicts that the intrinsic catalytic activities can be obtained from the linear slopes equal to α/σ. The values of α/σ obtained by linear fitting up to 70% conversion are in the range of 0.2 to 1.8. For sample *B* the parameters in Eq. 4 provide $\sigma = 51{,}100$ and in turn these values give relative catalytic activity α in the range of 10^4. It may be noted in comparison from Figures 3 and 4 that the overall reaction rates only increased some two to five times as catalyst was added to the system, that is, the increases of overall reaction rate were four orders of magnitude smaller than the increases in the intrinsic catalytic reactivities. This finding is consistent with the model under consideration, since a large fraction of the available reaction surface of the char is contained in the internal pore structures that were not exposed to the impregnating catalysts.

In view of the foregoing, one would expect that catalyst impregnation on porous chars would result in significantly smaller rate increases than otherwise comparable impregnation on nonporous carbons. This was in fact reported by McKee et al. (1983),

Table 2. Intrinsic Catalytic Rate Constants for Catalytic Char-Air Reactions

Sample	Catalyst	Impregnating Concentration (Molarity)	Intrinsic Catalytic Rate Constant $\times 10^4$, $\frac{\text{mol } C}{m^2 \cdot s} \times \frac{m^3}{\text{mol } O_2}$ Reaction temperatures, °C 380	400	430	455	480	500
A	Na_2CO_3	1.0	—	—	0.96	2.34	3.94	4.64
A	K_2CO_3	1.0	—	—	6.12	7.73	16.90	20.18
B	Na_2CO_3	0.2	2.02	3.96	6.55	—	—	—
B	Na_2CO_3	0.5	6.86	16.13	29.89	—	—	—
B	Na_2CO_3	1.0	10.71	23.07	39.31	—	—	—
B	Na_2CO_3	2.0	10.71	23.07	39.31	—	—	—
B	Na_2CO_3	3.0	10.71	23.07	39.31	—	—	—
B	K_2CO_3	0.2	5.46	7.35	16.79	—	—	—
B	K_2CO_3	0.5	14.26	26.13	45.86	—	—	—
B	K_2CO_3	1.0	22.28	36.24	70.84	—	—	—
C	Na_2CO_3	0.2	—	3.77	11.27	24.22	—	—
C	Na_2CO_3	0.5	—	5.18	13.24	37.04	—	—
C	Na_2CO_3	1.0	—	8.89	26.48	53.18	—	—
D	Na_2CO_3	0.2	—	2.47	6.81	14.31	—	—
D	Na_2CO_3	0.5	—	4.74	12.25	21.87	—	—
D	Na_2CO_3	1.0	—	6.51	18.79	27.59	—	—
E	Na_2CO_3	1.0	10.45	20.69	34.37	—	—	—
F	Na_2CO_3	1.0	8.26	12.87	25.52	—	—	—

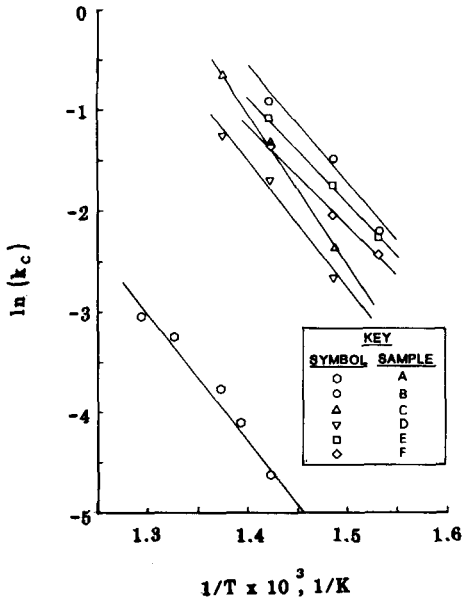

Figure 7. Catalytic rate constants for sample *A* to *F* impregnated with 1.0 M Na_2CO_3 solution.

TABLE 3. ACTIVATION ENERGY FOR CATALYTIC AND NONCATALYTIC CHAR-AIR REACTIONS

Sample	Catalyst	Concentration (Molarity)	Catalytic Activation Energy kcal/mol	Noncatalytic Activation Energy kcal/mol
A	Na_2CO_3	1.0	25.1 ± 4.2	23.5 ± 1.2
A	K_2CO_3	1.0	21.9 ± 6.3	
B	Na_2CO_3	0.2	21.6 ± 5.1	
B	Na_2CO_3	0.5	26.0 ± 5.7	21.5 ± 3.0
B	Na_2CO_3	1.0, 2.0, 3.0	23.2 ± 6.1	
B	K_2CO_3	0.2	21.5 ± 4.6	
B	K_2CO_3	0.5	22.1 ± 4.4	21.5 ± 3.0
B	K_2CO_3	1.0	20.9 ± 4.5	
C	Na_2CO_3	0.2	28.8 ± 4.3	
C	Na_2CO_3	0.5	32.4 ± 4.9	22.5 ± 2.2
C	Na_2CO_3	1.0	31.8 ± 3.2	
D	Na_2CO_3	0.2	29.0 ± 4.2	
D	Na_2CO_3	0.5	26.6 ± 4.3	22.5 ± 2.1
D	Na_2CO_3	1.0	25.0 ± 5.7	
E	Na_2CO_3	1.0	20.9 ± 2.8	26.5 ± 4.5
F	Na_2CO_3	1.0	20.0 ± 3.9	23.7 ± 4.3

who showed that addition of 10 wt. % of K_2CO_3 to lignite chars by ball milling produced an increase in reaction rate of only three to four times, while the same addition of catalyst to graphite increased the gasification rates by two to four orders of magnitude, a figure that is close to the intrinsic catalytic activity obtained in this study. Similarly, a study on the Pb-catalyzed oxidation of single crystal graphite by Harris et al. (1973) found that the ratio of catalyzed to uncatalyzed reaction rates, based on direct measurement on the edge recession of the graphite basal plane under a microscope, is in the range of 8.5×10^4 to 2.2×10^5, demonstrating again the significant difference between the intrinsic and overall catalytic rates.

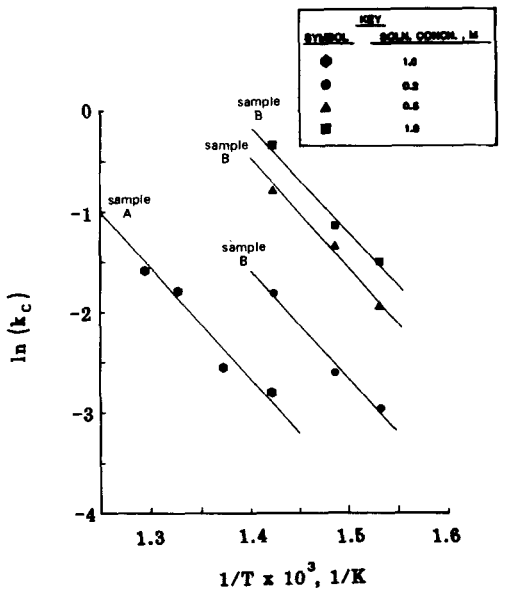

Figure 8. Catalytic rate constants for samples *A* and *B* impregnated with different concentrations of K_2CO_3 solution.

Also shown in Figures 1 to 4 are the model fits to the data computed by Eqs. 1 and 2 using the α values obtained by the previous analysis. The model describes the overall reaction kinetic behavior within ±20%, but mostly within ±10%. The reaction rates in the first 20% of conversion tend to be smaller than the model prediction, probably because of the time lag needed before the reactant gas can completely replace inert gas in the reaction chamber at the initiation of the reaction. The reaction rates at other temperatures and for the other impregnated chars all follow similar trends and are reported in full by Su (1983). The particle size parameters for the six chars studied are:

Char Sample	σ
A	35,900
B	51,100
C	51,600
D	34,100
E	45,300
F	34,600

These values were used with the model equations to estimate the intrinsic catalytic rates for each char. The results are summarized in Table 1.

Kinetic Parameters

The intrinsic catalytic rates may be characterized by the kinetic parameters: reaction order, activation energy, and preexponential factor. The effect of the catalysts on reaction order was determined in a set of isothermal experiments on sample *B* impregnated by 1.0 M Na_2CO_3 or K_2CO_3 solutions. The char was reacted at 673 K with oxygen ranging in a partial pressure from 5×10^3 to 2×10^4 Pa. The intrinsic catalytic oxidation was found to be a first-order reaction, as was earlier the case for noncatalytic oxidation (Su and Perlmutter, 1984). The addition of the catalysts does not affect the order of reaction, and the intrinsic catalytic rate constants can be obtained simply by dividing rates by corresponding oxygen concentrations. Catalytic rate constants obtained in this way are presented in Table 2 and shown on Arrhenius coordinates in Figures 7 and 8.

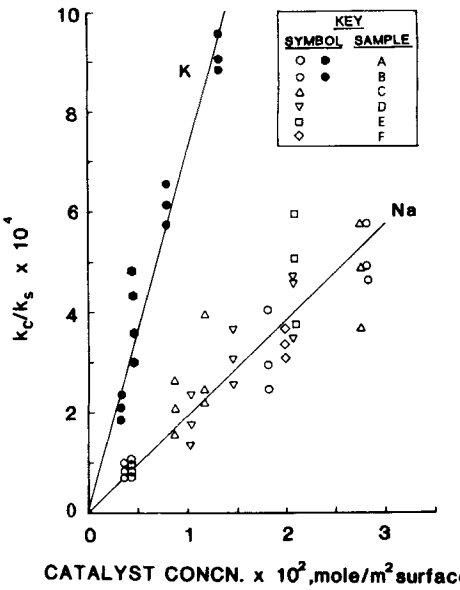

Figure 9. Correlation between the ratio of catalytic to noncatalytic rate constants and the catalyst surface concentration. Catalysts: K_2CO_3, filled points; Na_2CO_3, open points.

The computed activation energies are listed in Table 3 and compared to those for noncatalytic reactions (Su and Perlmutter, 1984). The activation energies of the catalytic reactions are not significantly different from those of noncatalytic reactions within a 90% confidence level, except for the Na_2CO_3-catalyzed sample *C*, which showed a slightly higher value of activation energy. The type of catalyst (Na or K) or the catalyst concentration does not affect the activation energies of the intrinsic reactions regardless of the source of the char (anthracite or bituminous).

Any attempt to compare these results with prior studies must remain inconclusive: although many authors have observed a decrease in activation energy on addition of the catalyst (Walker et al., 1966), there have been reports that the activation energy remained unchanged (Otto and Shelef, 1976) or even increased (Heintz and Parker, 1966). To some extent these discrepancies may be attributable to the use of reaction regimes that include diffusional resistance; in most cases the results use rates averaged over ranges of conversion without taking into account the finding of Heuchamps et al. (1965) to the effect that one can obtain different activation energies at different conversion levels. Most important of all, the activation energies obtained by using these overall catalytic rates do not represent the activation energy of the intrinsic catalytic reactions, since the overall rates are the combined effects of both catalytic and noncatalytic mechanisms.

Surface Concentrations

With an unchanged activation energy, the function of the catalyst is to increase the concentration of the reaction sites in the char surface. Since the catalysts reside only on particle exteriors, the catalyst surface concentations can be calculated from the known catalyst uptakes by assuming a spherical particle geometry. Further, the constancy in activation energy implies that the ratios of rate constants are equivalent to the ratios of the preexponential factors.

The ratios of the catalytic to noncatalytic rate constants obtained at various reaction temperatures were found to correlate linearly with the catalyst surface concentration shown in Figure 9. This figure is a composite of results at 400°C obtained from Figures 5 and 6 superimposed on other results (Su, 1983) measured at 430 and 455°C. Since k_c/k_s is equal to 1 without catalyst deposition, one obtains the empirical correlations:

$$k_c/k_s = 1 + 1.92 \times 10^6\,[\mathrm{Na}] \tag{5}$$

and

$$k_c/k_s = 1 + 7.18 \times 10^6\,[\mathrm{K}] \tag{6}$$

from the linear regressions of Figure 9, with correlation coefficients of 0.90 and 0.97, respectively. It should be noted that the unity intercepts are not distinguishable on the compressed scale of Figure 9.

The saturation effects that are often observed on catalyst uptakes and rate increase indicate that both [Na] and [K] should have certain upper limits at which all the carbon sites on a surface are covered by catalyst. Noting that increasing solution concentration higher than 1.0 M did not increase either the sodium uptake or rection rate for sample *B*, the upper limit of [Na] for this char is about 3.0×10^{-2} mol/m^2 (see Figure 9). This figure is inexact, since spherical geometry was used to approximate irregularly shaped particles. Furthermore, it involves parameters of catalyst dispersion and the size of catalyst particulates that are undetermined.

According to Eqs. 5 and 6, the intrinsic catalytic activity of K is four times larger than the activity of Na, even though the K_2CO_3-catalyzed chars showed only slightly higher overall rates than those catalyzed by Na_2CO_3 (see Figures 3 and 4). Since the activation energy of the reaction was unaffected by either catalyst, K_2CO_3 probably existed as smaller sizes of particulate on the char surface, thus creating more reaction sites than the same amount of the Na_2CO_3. It is noteworthy that the different chars tested in this study all fall on the same line in the correlations of Eqs. 5 and 6, including even sample *A* generated from the different parent coal.

Although there have been reports (Wood et al., 1981; Huhn et al., 1983; Mims and Pabst, 1983) that deposited catalysts may partially evaporate under gasification conditions, this does not appear to have occurred in these experiments. Table 4 compares the Na and K content of the impregnated char sample *B* before reaction with those of the completely reacted ash after oxidation at 673 K. The differences are within experimental error, suggesting that the impregnated catalysts were completely retained by chars during the subsequent oxidation reactions. This is consistent with a TGA experiment which showed that sodium and potassium carbonates did not undergo any appreciable decomposition or varporization under nitrogen or air atmospheres to at least 873 K. In fact, those studies that reported metal vaporizations are for potassium under CO_2, H_2O, or inert atmospheres (He, N_2, or vacuum) at higher temperatures (973 to 1,173 K). Sodium is usually regarded as less mobile than potassium due to its higher boiling point. Furthermore, when the gasification is under oxygen where active species are metal oxides, or at low pretreatment and gasifi-

TABLE 4. Na AND K CONTENT (IN WT %) OF IMPREGNATED CHAR SAMPLE B BEFORE AND AFTER SUBSEQUENT OXIDATION REACTION AT 400°C

Catalyst	Condition	Concentration of Impregnating Solution 0.2 M	0.5 M	1.0 M
Na_2CO_3	Before Reaction	0.21	1.00	1.55
	After Reaction	0.20	1.14	1.45
K_2CO_3	Before Reaction	0.32	0.73	1.23
	After Reaction	0.33	0.68	1.42

TABLE 5. COMPARISONS OF CATALYST UPTAKE FOR SINGLE AND MULTIPLE CATALYST IMPREGNATIONS ON CHAR SAMPLE B

Composition of Impregnating Solution		Catalyst Uptake in wt. % Char	
Molarity of Na_2CO_3	Molarity of K_2CO_3	Na	K
0.2	—	0.21	—
0.5	—	1.00	—
—	0.2	—	0.32
—	0.5	—	0.73
0.2	0.2	0.21	0.34
0.5	0.2	1.14	0.30
0.5	0.5	0.63	0.78

TABLE 6. CALCULATED CATALYTIC ACTIVITIES FOR SAMPLE B IMPREGNATED BY BOTH K_2CO_3 AND Na_2CO_3 SOLUTIONS

Composition of Impregnating Solution		$\frac{k_c}{k_s} \times 10^{-4}$		$\frac{\alpha}{\sigma}$		
Molarity of Na_2CO_3	Molarity of K_2CO_3	Na	K	Na	K	Total
0.2	0.2	0.74	2.37	0.15	0.46	0.61
0.5	0.2	4.01	2.09	0.78	0.41	1.19
0.5	0.5	2.22	6.02	0.43	1.18	1.61

cation temperatures, this vaporization phenomenon should not occur at all.

Multiple Catalysts

If two deposited catalysts each act to increase the concentation of reaction sites, the combined catalyst activity would be expected to show a simple additivity. To test this idea a set of experiments was conducted by impregnating char sample *B* (of 250 micron particle size) with an impregnating solution containing desired concentrations of both Na_2CO_3 and K_2CO_3. The atomic absorption data in Table 5 compare the catalyst uptakes for single and multiple catalyst impregnations. The existence of 0.2 M K_2CO_3 in 0.2 M or 0.5 M Na_2CO_3 solutions did not affect either sodium or potassium uptake as compared to single catalyst impregnations, indicating that the catalyst uptake had not reached the saturation limit. However, the existence of 0.5 M K_2CO_3 in 0.5 M Na_2CO_3 significantly reduced the sodium uptake without affecting potassium uptake, suggesting that the catalyst reached a saturation limit, with Na_2CO_3 a weaker contender than the more catalytically active K_2CO_3.

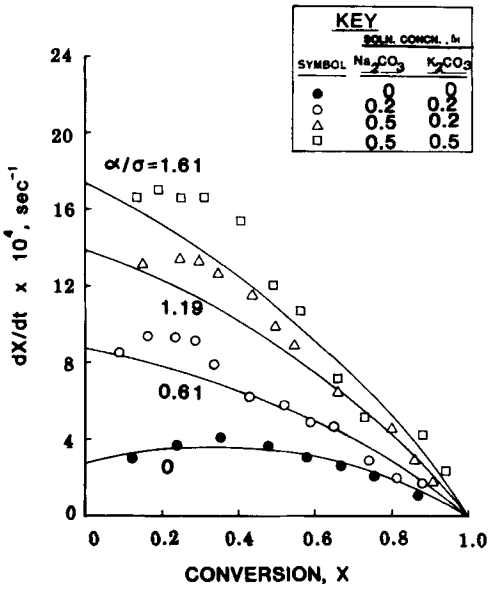

Figure 10. Char-air reaction rates for multiple-catalyzed sample *B* at 380°C; curves are the model predictions.

The values of k_c/k_s and α/σ for each catalyst were calculated from Eqs. 5 and 6. The results are shown in Table 6, together with the total catalytic activity obtained by adding the activities of each catalyst. The rates predicted by using these α/σ values are shown in Figure 10, superimposed on the measured oxidation rates of these multiple-catalyzed samples in air at 653 K. Although the predictions are slightly lower than the experimental results at early stages of conversion, the agreements are within ±20%, demonstrating the additivity of catalytic activities.

It should be noted that since overall rates are the combined contributions from catalytic and noncatalytic mechanisms, only the former part is affected by the dual catalyst enhancement. The noncatalytic contribution is the same whether a single or dual catalyst is used. This is shown in Figure 11 where curves 2 and 3 are the overall rates for chars impregnatd with single catalysts. When treated with multiple catalysts in the same amount, the experimental rate falls below the summation of curves 2 and 3 because both curves contain the noncatalytic rates which are not additive.

Changes in Pore Structure

A series of experiments was conducted to determine the pore surface area development of the catalyzed char. Char sample *B*

TABLE 7. SURFACE AREAS OF CHAR SAMPLE *B* AT DIFFERENT CONVERSION LEVELS
Areas are expressed in m^2/g of partially reacted sample.
Reactions were catalyzed by Na_2CO_3 or K_2CO_3 at 673 K.

Catalyst	Conc. of Impregnating Solution (Molarity)	Conversion, % 0	15	30	45	60	75
Non-catalytic	—	275	354	366	437	439	398
Na_2CO_3	0.2	275	330	355	390	383	382
	0.5	275	324	326	366	365	359
	1.0	275	284	314	349	347	338
K_2CO_3	0.2	275	334	378	414	440	424
	0.5	275	309	329	340	363	355
	1.0	275	287	306	326	333	329

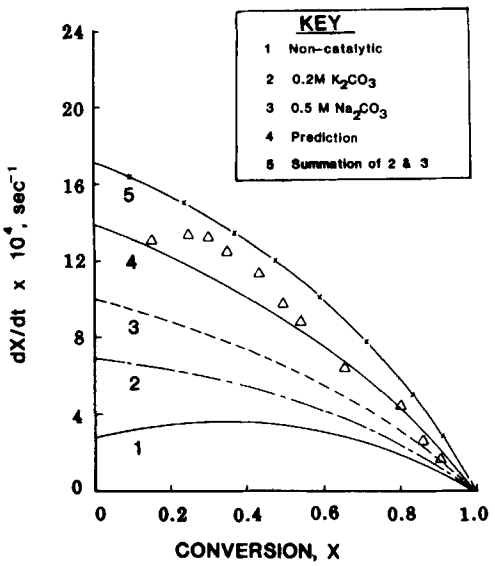

Figure 11. Comparisons of char-air reaction rates for single and multiple catalyzed sample *B* at 380°C. Catalysts: 0.2 M K_2CO_3; 0.5 M Na_2CO_3.

treated with either 0.2, 0.5, or 1.0 M solution of Na_2CO_3 or K_2CO_3 was reacted with air at 673 K to different levels of conversion (15, 30, 45, 60 and 75%). The surface areas of these partially reacted catalyzed samples, measured by adsorption of CO_2 at 273 K, are presented in Table 7. The initial pore structures of the unreacted chars were shown earlier (Su and Perlmutter, 1985) not to be affected by the impregnation with catalysts. The results in Table 7 show however that after partial conversion pore structures were less developed for those samples with greater catalyst uptake. As expected when catalytic enhancement exists only on the particle surfaces, the char is gasified relatively rapidly by catalytic reaction from the particle exterior, whereas the noncatalytic reaction within the pore structure is relatively less significant. The pore structure is therefore less affected by conversion than it would be in noncatalytic gasification, and the greatest differences in surface areas developed at the highest conversion levels.

Similar finding were reported by Wigmans et al. (1983), who showed that steam gasification of Ni-catalyzed activated carbon resulted in significantly smaller surface area than the gasification of the uncatalyzed sample. When they used K_2CO_3 as a catalyst, however, the surface area development was greater than for the uncatalyzed sample. Since the carbon sample used by these authors was able to be penetrated by catalyst solution, the reaction mechanisms involved are somewhat different from what is described in this study.

ACKNOWLEDGMENT

This research was funded by the U.S. Department of Energy Fossil Research Program under Contract No. EX 76-S-01-2450.

NOTATION

C_o = ambient concentrationof gas reactant, mol/^{3}
[K] = surface concentration of potassium on char particle, mol/m^2
k_c = catalytic rate constant for char surface reaction, in units that give m/s for $k_c C_o^m$
k_s = noncatalytic rate constant for char surface reaction, in units that give m/s for $k_s C_o^n$
L_o = total pore length per unit volume of unreacted particle, m/m^3
m = reaction order for catalytic reaction, dimensionless
n = reaction order for noncatalytic reaction, dimensionless
[Na] = surface concentration of sodium on char particle, mol/m^2
R = particle radius, m.
R_o = R at $t = 0$, m
S_o = total surface area per unit volume of unreacted particle, m^2/m^3
t = reaction time, s
X = conversion, dimensionless

Greek Letters

α = $k_c C_o^m / k_s C_o^n$ = ratio of catalytic to noncatalytic reaction rates
ϵ_o = initial porosity, dimensionless
σ = $R_o S_o/(1-\epsilon_o)$, a particle size parameter
τ = $k_s C_o t S_o\ (1-\tau_o)$, dimensionless time
ψ = $4\mu L_o(1-\epsilon_o)/S_o$, a pore structure parameter

LITERATURE CITED

Harris, P. S., F. S. Feates, and B. G. Reuben, "Controlled Atmosphere Electron Microscopic Studies of the Catalyzed Graphite-Oxygen Reaction. 2: The Influence of Lead," *Carbon*, **11**, 565 (1973).
Heintz, E. A., and W. E. Parker, "Catalytic Effect of Major Impurities on Graphite Oxidation," *Carbon*, **4**, 473 (1966).
Heuchamps, C., X. Duval, and M. Letort, "Evolution des Effets Catalytiques des Traces de Cendres au Cours de la Combustion du Graphite," *Compt. Rend.*, **260**, 1,160 (1965).
Huhn, F., J. Klein and H. Jüntgen, "Investigations on the Alkali-Catalyzed Steam Gasification of Coal: Kinetics and Interactions of Alkali Catalyst with Carbon," *Fuel*, **62**, 196 (1983).
McKee, D. W., et al. "Catalysis of Coal Char Gasification by Alkali Metal Salts," *Fuel*, **62**, 217 (1983).
Mims, C. A., and J. K. Pabst, "Role of Surface Salt Complexes in Alkali-Catalyzed Carbon Gasification," *Fuel*, **62**, 1,976 (1983).
Otto, K., and M. Shelef, "Catalytic Steam Gasification of Carbon: Effects of Ni and K on Specific Rates," *Proc. 6th Int. Cong. on Catalysis*, **2**, 1,082, The Chemical Society, Burlington House, London (1976).
Su, J. L., "Pore Structure and Catalyst Effects on Char Gasification Kinetics," Ph.D. Thesis, Univ. of Pennsylvania (1983).
Su, J. L., and D. D. Perlmutter, "Effect of Pore Structure on Char Oxidation Kinetics," *AIChE J.*, **31**, (1985).
Su, J. L. and D. D. Perlmutter, "Porosity Affects on Catalytic Char Oxidation. I: A Catalyst Deposition Model," *AIChE J.*, **31**, (1985).
Walker, Jr., P. L., M. Shelef, and R. A. Anderson, "Catalysis of Carbon Gasification," *Chemistry and Physics of Carbon*, **2**, 287, Marcel Dekker, New York (1966).
Wigmans, T., et al., "The Influence of Potassium Carbonate on Surface Area Development and Reactivity during Gasification of Activated Carbon by Carbon Dioxide," *Carbon*, **21**, 13 (1983).
Wood, B. J., et al., "The Mechanism of Catalytic Gasification of Coal Char," Technical Report No. 2, SRI International, DOE Contract No. DE-AC21-80MC14953 (Mar. 1981).

Manuscript received Apr. 3, 1984, and accepted Oct. 15.